Toward Engineering the Stability and Hemin-Binding Properties of Microsomal Cytochromes b_5 into Rat Outer Mitochondrial Membrane Cytochrome b_5: Examining the Influence of Residues 25 and 71[†]

Aaron B. Cowley,[‡] Adriana Altuve,[§] Olga Kuchment,[‡] Simon Terzyan,[||] Xuejun Zhang,[||] Mario Rivera,*[,§] and David R. Benson*[,‡]

Department of Chemistry, University of Kansas, Lawrence, Kansas 66045-7582, Department of Chemistry, Oklahoma State University, Stillwater, Oklahoma 74078-3071, and Crystallography Program, Oklahoma Medical Research Foundation, 825 NE 13th Street, Oklahoma City, Oklahoma 73104

Received April 23, 2002; Revised Manuscript Received July 23, 2002

ABSTRACT: As part of a larger effort to engineer the stability and hemin-binding properties of microsomal (Mc) cytochromes b_5 into rat liver outer mitochondrial membrane (OM) cytochrome (cyt) b_5, several mutants of rat OM cyt b_5 were prepared to study the effect of gradual and complete elimination of two extended hydrophobic networks, which are present in the structure of the mitochondrial protein and are absent in the structure of mammalian Mc cytochromes b_5. One of the hydrophobic networks, identified in a previous study [Altuve, A., Silchenko, S., Lee, K.-H., Kuczera, K., Terzyan, S., Zhang, X., Benson, D. R., and Rivera, M. (2001) *Biochemistry 40*, 9469−9483], encompasses the side chains of Ala-18, Ile-32, Leu-36, and Leu-47, whereas a second hydrophobic network, identified as part of this work, encompasses the side chains of Ile-25, Phe-58, Leu-71, and the heme. The X-ray structure of the A18S/I25L/I32L/L47R/L71S quintuple mutant of rat OM cyt b_5 demonstrates that both hydrophobic networks have been eliminated and that the corresponding structural elements of the Mc isoform have been introduced. The stability of the rat OM mutant proteins studied was found to decrease in the order wild type > I25L > A18S/I32L/L47R > L71S > A18S/I32L/L47R/L71S > 18S/I25L/I32L/L47R/L71S, indicating that the two hydrophobic networks do indeed contribute to the high stability of rat OM cyt b_5 relative to the bovine Mc isoform. Surprisingly, the quintuple mutant of rat OM cyt b_5 is less stable than bovine Mc cyt b_5, even though the former exhibits significantly slower rates of hemin release and hemin reorientation at pH 7.0. However, at pH 5.0 the bovine Mc and rat OM quintuple mutant proteins release hemin at comparable rates, suggesting that one or both of the His axial ligands in the rat OM protein are more resistant to protonation under physiological conditions. Results obtained from chemical denaturation experiments conducted with the apoproteins demonstrated that mutants containing L71S are significantly less stable than bovine Mc apocyt b_5, strongly suggesting that Leu-71 plays a pivotal role in the stabilization of rat OM apocyt b_5, presumably via hydrophobic interactions with Ile-25 and Phe-58. Because comparable interactions are absent in bovine Mc apocyt b_5, which contains Ser at position 71, it must resort to different interactions to stabilize its fold, thus highlighting yet another difference between rat OM and bovine Mc cyt b_5. During the course of these investigations we also discovered that rat OM cyt b_5 can be made to strongly favor hemin orientational isomer A (I32L) or isomer B (L71S) with a single point mutation and that release of hemin orientational isomers A and B can be kinetically resolved in certain rat OM mutants.

Two isoforms of cytochrome b_5 (cyt b_5)[1] have been identified in mammalian liver (*1, 2*). One is tail-anchored to the membrane of the endoplasmic reticulum (microsomal, or Mc cyt b_5), and the other is tail-anchored to the outer membrane of mitochondria (OM cyt b_5). Although rat OM cyt b_5 was originally identified nearly 30 years ago (*3*), nothing was known of its biophysical properties until a gene for the heme-binding domain was synthesized by Rivera et al. in 1992 (*4*). The sequence of this 92-residue recombinant protein is shown in Figure 1, aligned with the sequence of the tryptic fragment of bovine Mc cyt b_5 (*6*, *7*) and the corresponding sequences of other mammalian Mc cytochromes b_5 for which genes have been cloned (*6*, *8*−*12*). The numbering in Figure 1, which we employ throughout this paper, is based on the scheme initially introduced by Mathews for the lipase fragment of bovine Mc cyt b_5 (*5*). The full-length Mc proteins share 84−97% sequence identity and 93−98% sequence similarity, whereas the full-length bovine Mc and rat OM isoforms share only 49% sequence

[†] This work was supported by grants from the National Science Foundation (MCB-0110139 to D.R.B. and M.R.) and the National Institutes of Health (GM 50503 to M.R.).

* Correspondence should be addressed to these authors. D.R.B.: telephone, (785) 864-4090; telefax, (785) 864-5396; e-mail, drb@ku.edu. M.R.: telephone, (405) 744-5945; telefax, (405) 744-6007; e-mail, rivera@okstate.edu.

[‡] University of Kansas.

[§] Oklahoma State University.

[||] Oklahoma Medical Research Foundation.

[1] Abbreviations: cyt, cytochrome; Mc, microsomal; OM, outer membrane of mitochondria; Mb, myoglobin; GdmCl, guanidinium chloride; GdmSCN, guanidinium thiocyanate.

10.1021/bi026005l CCC: $22.00
Published on Web 08/31/2002

```
                  -1  1          11          21          31
Rat OM         DGQGS  DPAVTYYRLE  EVAKRNTAEE  TWMVIHGRVY  DITRFLSEHP
Bovine Mc            AVKYYTLE  EIQKHNNSKS  TWLILHYKVY  DLTKFLEEHP
Rabbit Mc            DVKYYTLE  EIKKHNHSKS  TWLILHHKVY  DLTKFLEEHP
Porcine Mc           AVKYYTLE  EIQKHNNSKS  TWLILHHKVY  DLTKFLEEHP
Mouse Mc             DVKYYTLE  EIQKHKDSKS  TWVILHHKVY  DLTKFLEEHP
Human Mc             AVKYYTLE  EIQKHNHSKS  TWLILHHKVY  DLTKFLEEHP
Rat Mc               DVKYYTLE  EIQKHKDSKS  TWVILHHKVY  DLTKFLEEHP

              41          51          61          71          81
Rat OM         GGEEVLIEQA  GADATESFED  VGHSPDAREM  IKQYYIGDVH  PNDLKPK
Bovine Mc      GGEEVLREQA  GGDATENFED  VGHSTDAREL  SKTFIIGELH  PDDR
Rabbit Mc      GGEEVLREQA  GGDATENFED  VGHSTDAREL  SKTFIIGELH  PDDR
Porcine Mc     GGEEVLREQA  GGDATENFED  VGHSTDAREL  SKTFIIGELH  PDDR
Mouse Mc       GGEEVLREQA  GGDATENFED  VGHSTDAREL  SKTYIIGELH  PDDR
Human Mc       GGEEVLREQA  GGDATENFED  VGHSTDAREM  SKTFIIGELH  PDDR
Rat Mc         GGEEVLREQA  GGDATENFED  VGHSTDAREL  SKTYIIGELH  PDDR
```

FIGURE 1: Amino acid sequence alignments of the recombinant heme-binding domain of rat OM cyt b_5, the tryptic fragment of bovine Mc cyt b_5, and the corresponding sequences of other mammalian Mc cytochromes b_5 for which genes have been cloned. Residues are numbered according to the scheme originally introduced by Mathews (*5*). Heme iron ligands His-39 and His-63 are shown in bold. Rat OM residues mutated as part of this work are highlighted with a black background. Residue −5 in the recombinant rat OM protein is Asp instead of Asn due to an error in the originally reported protein sequence (*2*).

identity and 68% sequence similarity (*13*). The X-ray crystal structures of the bovine Mc (*14*) and rat OM (*15*) proteins, however, demonstrate that the two isoforms share essentially identical folds. It is therefore striking that the reduction potential of the rat OM isoform (*16*−*18*) is approximately 100 mV more negative than the reduction potentials of the microsomal proteins (*19*−*22*). More recently, we have also shown that rat OM cyt b_5 exhibits considerably greater stability toward thermal and chemical denaturation than bovine Mc cyt b_5 and that the hemin-binding properties of rat OM cyt b_5 differ considerably from those of the Mc isoforms as well (*13*, *23*). For example, bovine Mc cyt b_5 releases hemin to apomyoglobin (apoMb) in aqueous solution at pH 7.0 (*24*), whereas rat OM cyt b_5 does not release hemin to apoMb at pH values as low as 5.2 (*13*, *23*). Furthermore, cytochromes b_5 are heterogeneous because the cofactor is bound in two different orientations, related to one another by a 180° rotation about the heme α,γ-meso axis (*25*). In all Mc isoforms where the isomers have been differentiated by ^{1}H NMR spectroscopy, the same isomer (referred to as isomer A) is found to predominate at equilibrium, but the ratio of major (A) and minor (B) isomers varies: 20:1 (A:B) in chicken (*26*), ∼9:1 (A:B) in rabbit (*25*) and bovine (*27*), and 1.6:1 (A:B) in rat Mc cyt b_5 (*26*). It is also known that in vitro reconstitution of the apoprotein with hemin initially results in the formation of a 1:1 ratio of A and B isomers. However, at room temperature these isomers undergo time-dependent changes in relative concentration until equilibrium is achieved ($t_{1/2} \sim 12$ h for bovine Mc cyt b_5 at 24 °C) (*20*, *27*). In contrast, rat OM cyt b_5 is isolated as a 1:1 mixture of hemin isomers (*4*) and remains thus even after prolonged incubation at 45 °C (*13*). Only after heating the protein at 65 °C for several hours does the hemin isomer ratio change, finally reaching equilibrium when A:B = 1:1.2 (*23*). Rat OM cyt b_5 thus represents the first documented example of a cyt b_5 exhibiting a thermodynamic preference for hemin isomer B and in which hemin is kinetically trapped under physiologically relevant conditions (*13*, *23*).

By comparing the crystal structures and sequences of rat OM and bovine Mc cyt b_5, we identified an extended hydrophobic patch in the rat OM protein that is absent in the bovine Mc isoform (*13*). This patch involves the side chains of Ala-18, Ile-32, Leu-36, and Leu-47. Ala-18 and Leu-47 engage in hydrophobic interactions at the protein surface; the side chain of Leu-47 forms an additional hydrophobic interaction with Leu-36 and also makes van der Waals contact with the side chain of Ile-32. By comparison, Ser-18 and Arg-47 in bovine Mc cyt b_5 (conserved among mammalian Mc cytochromes b_5; see Figure 1) form a hydrogen-bonding interaction at the protein surface, and although there is hydrophobic contact between the side chains of Arg-47 and Leu-36 in the Mc protein, no interactions are observed between the side chains of Leu-36 and Leu-32 (*13*). Experiments with the I32L, A18S/L47R, and A18S/I32L/L47R mutants of rat OM cyt b_5 indicated that protein stability diminished as the hydrophobic patch was disrupted (*13*). Complete disruption of the patch, which was verified in a 2.0 Å crystal structure of the A18S/I32L/L47R mutant (PDB code: 1ICC), also facilitated hemin reorientation and hemin release. Nonetheless, hemin is still kinetically trapped in the A18S/I32L/L47R triple mutant under physiological conditions, and the protein remains considerably more stable toward thermal and chemical denaturation than the bovine Mc isoform. In addition, NMR studies carried out with these mutants revealed that replacing Ile-32 with Leu alters the thermodynamic equilibrium of hemin orientational isomers, which changes from 1:1.2 (A:B) in wild-type OM cyt b_5 to 1:4.0 (A:B) in the I32L and A18S/I32L/L47R mutants (*13*).

Subsequent comparisons of amino acid sequences and X-ray crystal structures allowed us to identify Leu-71 and Ile-25 as two additional residues which might contribute to the unusual properties of rat OM cyt b_5 relative to the Mc isoforms. The corresponding residues in bovine Mc cyt b_5 are Ser-71 and Leu-25, which are conserved among mammalian Mc cytochromes b_5 (Figure 1). The side chains of Leu-71 and Ile-25 in rat OM cyt b_5 make van der Waals contact with one another as well as with heme, suggesting the presence of a second hydrophobic network in the rat OM protein which might contribute to stabilizing it relative to the Mc isoforms. Consequently, replacing Leu-71 and Ile-25 in rat OM cyt b_5 with the corresponding residues in Mc cyt b_5 was expected to exert a significant influence on the stability and hemin-binding properties of the protein. In fact, we find that the A18S/I32L/L47R/I25L/L71S mutant of rat

OM cyt b_5, in which both hydrophobic networks unique to the wild-type protein have been disrupted, is less stable toward chemical denaturation than wild-type bovine Mc cyt b_5. However, at pH 7.0 the quintuple mutant exhibits rates of hemin reorientation and hemin release that are significantly lower than those measured for bovine Mc cyt b_5.

EXPERIMENTAL PROCEDURES

General. Recombinant rat liver OM cyt b_5, bovine Mc cyt b_5, and the site-directed mutants studied in this work were expressed in *Escherichia coli* BL21(DE3) and purified as described previously (*4*). Single-stranded oligonucleotides were synthesized by the Recombinant DNA/Protein Facility at Oklahoma State University.

Site-Directed Mutagenesis. The recombinant pET11a plasmid and the QuikChange site-directed mutagenesis kit (Stratagene) were used to construct all of the rat OM cyt b_5 mutants. The A18S/I32L/L47R/L71S quadruple mutant was constructed from the recombinant pET11a plasmid harboring the gene coding for the A18S/I32L/L47R triple mutant (*13*). The sequences corresponding to the mutagenic primers designed to introduce the L71S mutation are 5′-CCGGATGCGCGTGAAATGTCTAAACAGTACTACATCGGCG-3′ and 5′-CGCCGATGTAGTACTGTTTAGACATTTCACGCGCATCCGG-3′. The underlined codons represent mismatches introduced to generate the mutations. These same primers and the recombinant pET11a plasmid harboring the gene coding for wild-type rat OM cyt b_5 (*4*) were used to construct the L71S single point mutant. The A18S/I25L/I32L/L47R/L71S quintuple mutant was constructed from the recombinant pET11a plasmid harboring the gene coding for the A18S/I32L/L47R/L71S quadruple mutant. The sequences corresponding to the mutagenic primers designed to introduce the I25L mutation are 5′-GAAGAAACCTGGATGGTTCTGCATGGCCGTGTTTACG-3′ and 5′-CGTAAACACGGCCATGCAGAACCATCCAGGTTTCTTC-3′. The I25L mutant was constructed with these primers and the pET11a plasmid containing the WT rat OM cyt b_5 gene. The recombinant constructs were transformed into *E. coli* XL1 blue competent cells for amplification. Once the mutations had been confirmed by sequencing, the recombinant plasmids were transformed into *E. coli* BL21(DE3) cells for subsequent protein expression, which was carried out according to a previously described protocol (*4*).

Subcloning Bovine Mc Cytochrome b_5 into the pET11a Vector. The recombinant pUC19 plasmid, harboring the gene coding for the tryptic fragment of bovine Mc cyt b_5 (*28*), is a generous gift from Dr. Grant Mauk. The Mc cyt b_5 gene, including the ribosome-binding site (RBS), was excised by treatment with *Nde*I, followed by Mung bean nuclease to produce a blunt end, and subsequently restricted with *Xba*I. The pET11a vector was restricted with *Eco*RI, followed by treatment with Mung bean nuclease, and then digested with *Xba*I. The excised gene and the linearized plasmid were purified by agarose gel electrophoresis and extracted from the agarose gel with the aid of the Wizard PCR Preps DNA purification system (Promega), ligated with T4 DNA ligase, and the recombinant plasmid was transformed into *E. coli* XL1 blue cells for amplification and sequencing. Once the sequence of the gene had been established, the recombinant pET11a plasmids were transformed into *E. coli* BL21(DE3) cells for subsequent protein expression. Bovine Mc cyt b_5 was expressed and purified using a protocol previously described for the expression and purification of rat OM cyt b_5 (*4*).

^{1}H NMR Spectroscopy. ^{1}H NMR spectra were recorded on Varian Unity Inova NMR spectrometers operating at 399.97 and 598.658 MHz, ^{1}H frequency. Protein solutions were exchanged with perdeuterated sodium phosphate buffer (μ = 0.1 M, pH 7.0, not corrected for the isotope effect). All NMR samples had a volume of 0.8 mL and a protein concentration of ~3 mM. Spectra were acquired with water presaturation, 256 scans over a 30 kHz spectral width, 0.4 s acquisition time, and 1.0 s relaxation delay. Rate constants for hemin isomer interconversion were obtained by monitoring the time-dependent changes in the areas under the hemin resonances corresponding to isomers A and B as described previously (*20*, *29*). The equilibrium constant was obtained from the NMR spectrum when the hemin interconversion reaction reached equilibrium.

Thermal Denaturation Studies. Thermal denaturation experiments were performed on a Varian Carey 100 Bio UV/visible spectrophotometer outfitted with a Peltier-thermostated cell holder. Temperature was monitored within the cell using a dedicated temperature probe accessory (±0.1 °C). Sample concentrations ranged from 3 to 5 μM in 50 mM potassium phosphate, buffered to pH 7.0. The temperature was increased in increments of 2 °C, and samples were equilibrated for 5 min after reaching each desired temperature. The midpoint of thermal denaturation (T_m) was determined from the first derivative of a plot of Soret band absorbance at 412 nm (λ_{max}) vs temperature.

Chemical Denaturation Studies. Stock solutions of guanidinium chloride (GdmCl; Aldrich) or guanidinium thiocyanate (GdmSCN; Sigma) were prepared in 30 mM MOPS, buffered to pH 7.0. To eliminate potential errors due to weighing of the hygroscopic denaturants, stock solution concentrations were verified from measurements of the solution refractive index. Titrations monitored by electronic absorption spectroscopy were performed on the instrument described above with protein concentrations of 3−4 μM, following the change in absorbance at the Soret band λ_{max}. Fluorescence measurements were performed on a PTI QuantaMaster luminescence spectrometer with protein concentrations of 0.5−1 μM by monitoring fluorescence intensity at 340 nm after excitation at 280 nm. All solutions were incubated at 25 °C for 1 h before spectra were recorded at the same temperature. Denaturation curves were fit to eq 1 using the program Kaleidagraph (version 3.5), where ΔG^{H_2O} is the free energy of unfolding in the absence of denaturant, [D] is the concentration of denaturant, and m is a parameter indicating the sensitivity of the free energy of unfolding to denaturant concentration (*30*, *31*). The concentration of denaturant at which the protein is 50% denatured (C_m value) was calculated using eq 2.

$$\text{fraction folded} = \exp\{(\Delta G^{H_2O} - m[D])/RT\}/\{1 + (\Delta G^{H_2O} - m[D])/RT\} \quad (1)$$

$$\Delta G^{H_2O} = C_m m \quad (2)$$

Hemin Transfer Experiments. Horse skeletal apomyoglobin (apoMb) was employed as the receiving protein in hemin

transfer experiments. Removal of heme from the holoprotein (Calbiochem) was accomplished using the method of Teale (*32*). For measurements at pH 5.0, the solution was buffered with 150 mM sodium acetate. For experiments at pH 6.0 and 7.0, 150 mM potassium phosphate buffer was employed. All solutions contained 450 mM sucrose to help to stabilize the apoproteins (*33*). ApoMb concentrations were estimated using an extinction coefficient of 16.0 mM^{-1} cm^{-1} at 280 nm (*34*). In a typical hemin transfer experiment, a 1 mL solution of apoMb (40−60 μM) in the appropriate buffer solution was equilibrated at 37 °C in a 1.0 cm cuvette in the UV/vis spectrophotometer described above. A solution of the appropriate cyt b_5 prepared in the same buffer ($\leq$5 μL; final cyt b_5 concentration 2−4 μM) was added to the apoMb solution, and the absorbance at 406 nm (A_{406}) was monitored as a function of time. In most experiments, the concentration of apoMb was 18−25-fold greater than the concentration of cyt b_5. However, in experiments with the L71S and A18S/I32L/L47R mutants at pH 5.0 (which required more than 16 h to reach completion), protein precipitation was observed to occur if the apoMb to cyt b_5 ratio exceeded 10:1. Therefore, a 10:1 ratio of apoMb to cyt b_5 was used for determining hemin transfer rate constants for these mutants at pH 5.0. In experiments performed by recording spectra as a function of time for the A18S/I32L/L47R, L71S, and A18S/I32L/L47R/L71S mutants at pH 5.0 (with the sample zeroed at 700 nm before each scan), we observed that variation in absorbance at 415 nm was small (<4%) in comparison with that at 406 nm and largely random. During experiments in which the absorbance at 406 nm was recorded as a function of time, some drift of the signal occurred throughout the reactions. As a means of correcting for this drift, we also recorded the absorbance at 415 nm for these mutants and subsequently subtracted it from the absorbance at 406 nm. Because 415 nm likely does not represent a true isosbestic point due to the biphasic nature of the reactions (see Results and Discussion), it is possible that this correction process will lead to small errors in the fitted rate constants. However, we feel that the substantially improved fits of the data resulting from subtraction of the absorbance at 415 nm justify use of the procedure. For samples exhibiting extremely slow hemin transfer (k_{-H} < 0.1 h^{-1}), rate constants were estimated from initial rate data as previously described (*13*). For samples exhibiting faster hemin transfer, rate constants were obtained from plots correlating absorbance at A_{406} and time using the curve-fitting program Igor Pro (version 4.0, WaveMetrics, Inc.).

Crystallization and X-ray Diffraction Data Collection. The recombinant A18S/I25L/I32L/L47R/L71S quintuple mutant of rat OM cyt b_5 was concentrated to ~9 mg/mL in a buffer containing 20 mM Tris-HCl, pH 7.2. Crystals were grown in vapor diffusion plates at 278 K from hanging drops of the protein solution mixed 1:1 with the reservoir solution containing 32% (w/v) poly(ethylene glycol), 0.2 M magnesium acetate, and 0.1 M PIPES, pH 6.5. The typical size of a crystal was about 0.2 mm × 0.2 mm × 0.2 mm. Data collection was performed as previously described (*13*). A complete data set was collected up to 2.0 Å resolution.

Structural Determination and Refinement. The crystal structure of the rat OM cyt b_5 A18S/I25L/I32L/L47R/L71S quintuple mutant is isomorphous with that of the A18S/I32L/L47R triple mutant reported previously (*13*). One crystallographic asymmetric unit contains four cyt b_5 molecules with 44% solvent content. Refinement was carried out using the program CNS (version 1.0) (*35*) with 6% of the total reflections randomly selected prior to the refinement to monitor the R_{free} factor. Simulated annealing (from 5000 K) was used at the initial stage of the refinement to reduce bias of the template model. The graphics program FRODO (Turbo) (*36*) was used for interactive modeling. A default tight restriction on the planarity of heme groups was applied at early stages of refinement and was released to the level equivalent to aromatic rings of side chains of the protein. Coordinates of the crystal structure of the A18S/I25L/I32L/L47R/L71S mutant of cyt b_5 reported here have been deposited in the Protein Data Bank with accession code 1LJ0.

RESULTS AND DISCUSSION

Identification of a Second Hydrophobic Patch in Rat OM Cyt b_5. Disruption of the hydrophobic patch involving Ala-18, Ile-32, Leu-36, and Leu-47 in rat OM cyt b_5 destabilized the protein, as evidenced in thermal and chemical denaturation studies of the A18S/I32L/L47R triple mutant, and facilitated hemin transfer and reorientation (*13*). However, the triple mutant remains considerably more stable than bovine Mc cyt b_5, and hemin is still kinetically trapped under physiological conditions. Consequently, we attempted to identify additional differences between the rat OM and bovine Mc proteins that might account for their disparate stability and hemin-binding properties. Thus, detailed comparisons between their amino acid sequences and crystal structures (Figure 2) drew our attention to residue 71, which is located in the last (C-terminal) turn of one of the four α-helices surrounding the heme. In bovine Mc cyt b_5 residue 71 is a Ser (green in Figure 2A), whereas in the rat OM protein it is a Leu (green in Figure 2B). In the crystal structure of bovine Mc cyt b_5, the hydroxyl group on the side chain of Ser-71 is directed toward the solvent where it is involved in a network of hydrogen bonds with crystallographic water molecules, whereas the β-methylene group makes van der Waals contact with the heme methyl and heme vinyl substituents on pyrrole ring I, at the base of the heme-binding pocket (Figure 2A). Further inspection of the microenvironment surrounding Ser-71 in bovine Mc cyt b_5 revealed that a significant portion of the heme (red in Figure 2A) is exposed to the aqueous environment, as is evident from the unencumbered view of a significant portion of pyrrole ring I and of the vinyl group attached to it. By comparison, a similar view of rat OM cyt b_5 reveals that the corresponding heme pyrrole ring and its substituents are inaccessible to solvent. This stems largely from the fact that Leu-71 in rat OM cyt b_5 (green in Figure 2B) creates a very different microenvironment than does Ser-71 in bovine Mc cyt b_5. For example, one δ-methyl group of Leu-71 makes hydrophobic contact with the methyl and vinyl groups on nearby heme pyrrole ring I, while the other interacts with the side chain of invariant residue Phe-58 (blue).

In addition, both δ-methyl groups of Leu-71 make van der Waals contact with the δ-methyl group of Ile-25 (light blue), which also contacts the vinyl group on pyrrole ring I.[2] Finally, there is extensive packing between the side chains of Ile-25 and Phe-58, with the side chain of the latter engaging in edge-to-face aromatic stacking interactions with the heme macrocycle. Thus, the heme cofactor and the side

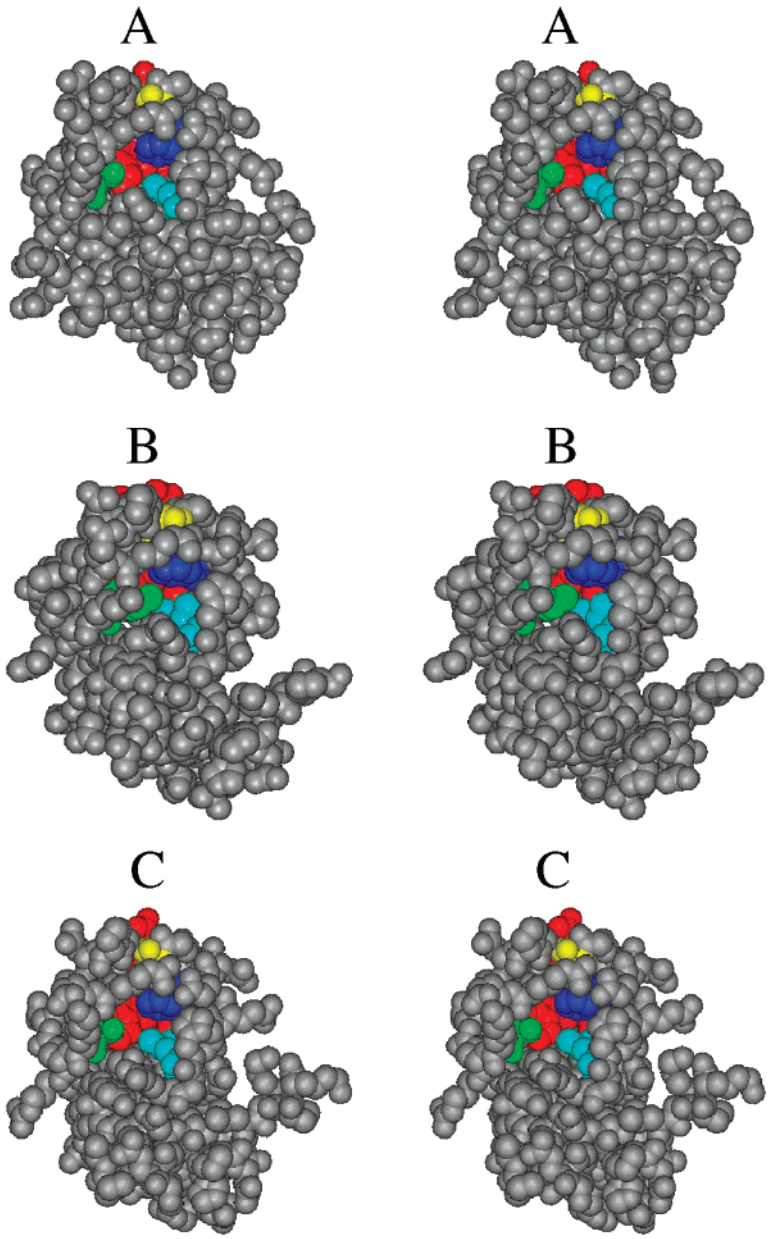

FIGURE 2: Space-filling stereo representations of the X-ray crystal structures of (A) bovine Mc cyt b_5, (B) wild-type rat OM cyt b_5, and (C) the A18S/I25L/I32L/L47R/L71S quintuple mutant of rat OM cyt b_5. In all structures heme is in red, axial ligands His-39 and His-63 are in yellow, residue 71 is in green, residue 25 is in light blue, and residue 58 is in blue.

chains of Leu-71, Ile-25, and Phe-58 comprise an extensive network of hydrophobic interactions.

Less extensive hydrophobic interactions are present in bovine Mc cyt b_5, which contains Leu at position 25 (light blue in Figure 2A). As with Ile-25 in the rat OM protein, Leu-25 in bovine Mc cyt b_5 interacts with the heme−vinyl group on pyrrole ring I and with the side chain of Phe-58 (blue). However, interactions between Ser-71 and Leu-25 and between Ser-71 and Phe-58 are absent. A consequence of the limited hydrophobic interactions among these residues is the formation of a relatively large cavity that exposes a section of the heme in Mc cyt b_5 to the aqueous environment. Two additional interactions involving Phe-58 are noteworthy: (i) its phenyl side chain is π-stacked against the imidazolyl side chain of heme ligand His-63, and (ii) its carbonyl oxygen provides a hydrogen bond to the NH group on the His-63 side chain. It is therefore conceivable that subtle differences in the microenvironment surrounding Phe-58 in rat OM cyt b_5 and bovine Mc cyt b_5 may influence the strength of the bond between His-63 and Fe(III), thereby modulating protein stability and propensity of the protein to release hemin. We therefore hypothesized that the more extensive hydrophobic network in the vicinity of Leu-71 and Ile-25 in rat OM cyt b_5 contributes to its greater stability and lower rates of hemin release and hemin reorientation in comparison to the bovine Mc protein. To probe this hypothesis, we prepared two mutants of rat OM cyt b_5 (L71S and I25L) in which Leu-71 and Ile-25 are replaced with the corresponding residues in the Mc proteins. In addition, we prepared the A18S/I32L/L47R/L71S quadruple and A18S/I25L/I32L/L47R/L71S quintuple mutants in order to probe

[2] It is important to note that the hemin orientational isomers are present in a 1:1 ratio in the wild-type protein used for crystallographic analysis, even though only one isomer (isomer A) was employed in refining the structure. In isomer B, a heme methyl group would reside near the side chain of Ile-25.

Table 1: Data Collection and Refinement Statistics

data statistics	
space group	$P2_12_12_1$
unit cell (Å)	$a = 39.8$
	$b = 50.9$
	$c = 167.4$
resolution (Å)	50.0−2.0
R_{merge} (%)	0.08 (0.37)[a]
no. of reflections	23729 (2215)
completeness (%)	99.2 (94.7)
$I/\sigma(I)$	22 (3.2)
refinement statistics	
$R_{working}$ (%)	21.0 (for 20088 reflections)[b]
R_{free} (%)	25.1 (for 1474 reflections)[b]
no. of non-hydrogen atoms	
protein (including heme)	2997
solvent	194
rmsd from ideal values	
bond length (Å)	0.015
bond angle (deg)	1.61
average *B*-factor (Å^2)	
protein	34.5
solvent	38.6

[a] Numbers in parentheses are the corresponding numbers for the highest resolution shell (2.1−2.0 Å). The highest resolution shell with R_{merge} below 20% is that corresponding to 2.4−2.25 Å. [b] Reflections of $|F_o| > 0.0$.

the effect of simultaneously disrupting the hydrophobic networks formed by Ala-18, Ile-32, Leu-36, and Leu-47 and by Ile-25, Phe-58, Leu-71, and the heme on the chemical and physical properties of rat OM cyt b_5. Insights obtained from the study of these proteins are described in the following sections.

X-ray Crystal Structure of the A18S/I25L/I32L/L47R/L71S Quintuple Mutant. Crystals of the A18S/I25L/I32L/L47R/L71S quintuple mutant were grown using conditions identical to those recently reported for crystallization of the A18S/I32L/L47R triple mutant. The 2.0 Å resolution structure has been refined to an *R*-factor of 21.0%, with an R_{free} of 25.1%. Table 1 reports the statistics of the diffraction data and the refinement statistics. As with the triple mutant, there are four cyt b_5 molecules per crystallographic asymmetric unit cell. The root-mean-square (rms) deviations between the Cα atoms (residues 4−85) of each possible pair of protein molecules in the asymmetric unit cell range between 0.37 and 0.43 Å, indicating that all four structures are essentially identical. The main differences between the four molecules are located at the N-temini. All of the mutated residues display good electron density, providing structural confirmation for the changes. Because ^{1}H NMR studies had demonstrated that isomer B is favored in the A18S/I32L/L47R triple mutant, isomer B was used in refining its crystal structure (*13*). Maps of the A18S/I25L/I32L/L47R/L71S quintuple mutant calculated using the structure of the triple mutant as a model show additional positive electron density close to the methyl groups of pyrrole rings I and II and negative electron density close to the vinyl groups, thus indicating that in the quintuple mutant hemin isomer A is favored. The final model of the A18S/I25L/I32L/L47R/L71S quintuple mutant contains heme in this orientation.

In terms of overall fold, the A18S/I25L/I32L/L47R/L71S quintuple mutant is identical to the wild-type (*15*) and A18S/I32L/L47R mutant (*13*) proteins. The side chain of Ser-71 (green in Figure 2C) adopts an orientation essentially identical to that of Ser-71 in bovine Mc cyt b_5, with the side-chain OH group oriented toward the aqueous environment, although there is no evidence that the OH group engages in hydrogen-bonding interactions with crystallographic water molecules, as was observed in the crystal structure of bovine Mc cyt b_5 (*14*). The structure of the quintuple mutant confirms that the structural microenvironment in the neighborhood of Ser-71 is very similar to that seen in Mc cyt b_5 in that a cavity exposes a sizable portion of pyrrole ring I and its vinyl substituent to the aqueous environment. As is the case with the Mc isoform, the structure of the quintuple mutant reveals an interaction between the β-methylene group of Ser-71 and the nearby heme vinyl group and a Leu-25 side chain exhibiting torsional angles nearly identical to those of Leu-25 in bovine Mc cyt b_5. It is therefore clear that replacing Ile-25 and Leu-71 with Leu and Ser, respectively, reproduces the corresponding structural microenvironment of bovine Mc cyt b_5 in the vicinity of residue 71. Moreover, the structure of the quintuple mutant confirms that the extended hydrophobic network encompassing Ala-18, Ile-32, Leu-36, and Leu-47 has also been disrupted. The crystal structure is therefore a useful aid in understanding the results of the biophysical studies described below.

Table 2: Hemin Orientational Isomer Ratios and Rates of Hemin Reorientation at pH 7.0

protein	hemin isomer ratio (A:B) as isolated	hemin isomer ratio (A:B) at equilibrium	k_1[a] (h^{-1})	$t_{1/2}$ (h)
wild-type rat OM	1:1	1:1.2[b]	*e*	*e*
I25L	1:1	1:1.1[c]	*e*	*e*
A18S/I32L/L47R	1:1	1:4.0[c]	0.05	13.9
L71S	1:1	5.2:1[c]	0.09	7.8
A18S/I32L/L47R/L71S	1.2:1	2.5:1[c]	0.24	2.8
A18S/I25L/I32L/L47R/L71S	1.2:1	1.5:1[c]	0.29	2.4
bovine Mc tryptic fragment	2.8:1	9:1[d]	*f*	*f*

[a] Determined at 45 °C. [b] Determined at 65 °C. [c] Determined at 45 °C. [d] Determined at 24 °C (*20*). [e] Too slow to measure. [f] Too fast to measure.

Effect of Mutagenesis on Hemin Orientational Isomer Ratio. The ratio of hemin orientational isomers in wild-type rat OM cyt b_5 and most of the mutants discussed in this paper is A:B = 1:1 following expression in *E. coli* (Table 2). This phenomenon is likely a consequence of freshly synthesized polypeptide (apoprotein) binding hemin in both orientations at identical rates during protein expression in the bacterial host. The isomer ratio remains 1:1 throughout the process of expression and purification because hemin is kinetically trapped at 37 °C. However, after heating each protein to an appropriate temperature, the thermodynamic equilibrium is attained. For example, heating the wild-type protein to 65 °C for 7 h resulted in a hemin orientational isomer ratio of A:B = 1:1.2 (Table 2) (*23*), while heating the A18S/I32L/L47R and I32L mutants to the same temperature resulted in an equilibrium ratio of A:B = 1:4.0 (*13*). The ^{1}H NMR spectrum obtained from the A18S/I32L/L47R mutant following hemin isomer equilibration is shown in Figure 3A. On the other hand, the isomer ratio obtained for the quadruple and quintuple mutants, immediately after expression and purification, is not 1:1 but rather A:B = 1.2:1. This observation suggests that these two mutants tend to approach their thermodynamic equilibrium (2.5:1 and 1.5:1, respectively) during protein expression, thereby indicating that hemin is no longer kinetically trapped at 37 °C. Insights

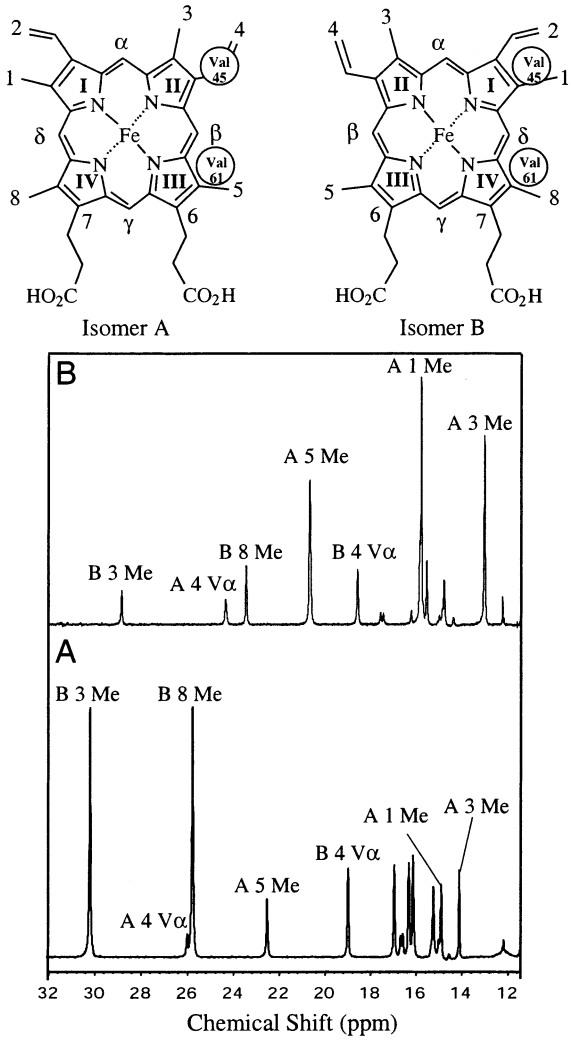

FIGURE 3: ^{1}H NMR spectra of the A18S/I32L/L47R (A) and L71S (B) mutants of rat OM cyt b_5 obtained after equilibrating the hemin orientational isomers at 45 °C for 50 h. The structures at the top of the figure indicate the numbering scheme used for the heme substituents in the two isomers that differ by a 180° rotation about the α,γ-meso axis.

gained from studying the kinetics of hemin release and hemin reorientation of these mutants will be discussed in the following section.

Studies conducted with the I32L and A18S/L47R/I32L mutants of rat OM cyt b_5 allowed us to conclude that residue 32 plays a key role in controlling the equilibrium position of isomers A and B, because both mutants exhibit an equilibrium ratio of A:B = 1:4 (*13*). The increased stability of isomer B was attributed to the fact that the two δ-CH_3 groups on the isobutyl side chain of Leu-32 (light blue in Figure 4A) pack against the methyl group located at position 3 of pyrrole ring I in isomer B (B 3Me; see Figure 3), thus restricting the space available at the bottom of the heme-binding pocket (*13*). The space available for the heme to place a vinyl group at this position (isomer A) is further restricted by the fact that one of the δ-CH_3 groups in the side chain of Leu-71 (blue in Figure 4A) packs against the heme. Hence, it is likely that a vinyl group at this position (position 2 in isomer A) will encounter energetically unfavorable interactions with the side chains of Leu-32 and Leu-71. In contrast, when Leu-71 is replaced by Ser and the resultant protein is allowed to reach equilibrium by heating it to 45 °C, isomer A is favored (A:B = 5.2:1), as can be seen from the corresponding ^{1}H NMR spectrum (Figure 3B). Stabilization of isomer A relative to isomer B in the L71S mutant is likely a consequence of increased room at the bottom of the heme pocket that accommodates a vinyl group at position 2 in pyrrole ring I of isomer A (A 2V; see Figure 3). Increased room at the bottom of the heme pocket is created by the shorter side chain of Ser and by the conformation of the Ile side chain, which directs the lone δ-CH_3 group away from the heme. These findings show that it is possible to select, at will, a mutant of rat OM cyt b_5 wherein isomer A or isomer B predominates. Remarkably, this can be achieved by introduction of a single point mutation: I32L "dials in" isomer B, whereas L71S "dials in" isomer A. This is, to the best of our knowledge, the first reported example in which the hemin isomer equilibrium has been completely reversed in a cytochrome *b*.

A second noteworthy observation regarding the equilibrium position of hemin isomerism in the different mutants investigated in this work stems from the finding that the A18S/I25L/I32L/L47R/L71S quintuple mutant displays an equilibrium ratio of A:B = 1.5:1, similar to that observed in rat Mc cyt b_5 (A:B = 1.6:1) (*26*) but clearly distinct from the A:B ≈ 9:1 displayed by bovine Mc cyt b_5 (*27*) and by the corresponding human protein (*37*). Comparing the sequence of the heme-binding domain of the rat OM quintuple mutant with the corresponding sequences of bovine, human, and rat Mc cyt b_5 (Figure 5), we find that they differ at a variety of positions. Much of the sequence divergence involves residues distant from the heme, for example, those located at the N- and C-termini, and therefore not likely to contribute directly to the hemin isomer ratio. In contrast, the side chains of residues 23, 70, and 74 (underlined in Figure 5) are situated near the heme. For example, the phenyl side chain of Phe-74 makes van der Waals contact with the methyl and vinyl groups on heme pyrrole ring I. Mortuza and Whitford found that replacing Phe-74 in bovine Mc cyt b_5 with Tyr, which occupies position 74 in rat Mc cyt b_5 and in the rat OM quintuple mutant, resulted in a change in hemin orientational isomer ratio from A:B ≈ 9:1 to A:B = 3.5:1 (note that Mortuza and Whitford employ an alternate numbering system in their report, with Phe-74 denoted as Phe-78) (*38*). Replacing Tyr-74 in the quintuple mutant of rat OM cyt b_5 is therefore likely to exert the opposite effect, increasing the population of isomer A at the expense of isomer B.

The side chain of Leu-23 in bovine Mc cyt b_5 makes contact with the methyl group of pyrrole ring II (isomer A). Mortuza and Whitford (*38*) demonstrated that replacing Leu-23 in bovine Mc cyt b_5 with Val, the corresponding residue in the rat Mc protein (see Figure 5), decreased the hemin isomer ratio (from A:B ≈ 9:1 to A:B = 4.0:1) by providing more room for a vinyl group to occupy the corresponding position, thereby increasing the population of isomer B at the expense of isomer A. It is also noteworthy that NMR studies conducted by Bertini and co-workers implicate residues 23 and 74 as important in modulating the predominance of isomer A in Mc cytochromes b_5 (*39*). Moreover, NMR spectroscopic studies carried out by La Mar and co-workers (*40*) also identified residue 23 as key to favoring isomer A in microsomal bovine cyt b_5. Residue 23 in the rat OM quintuple mutant is a Met whose side-chain methyl

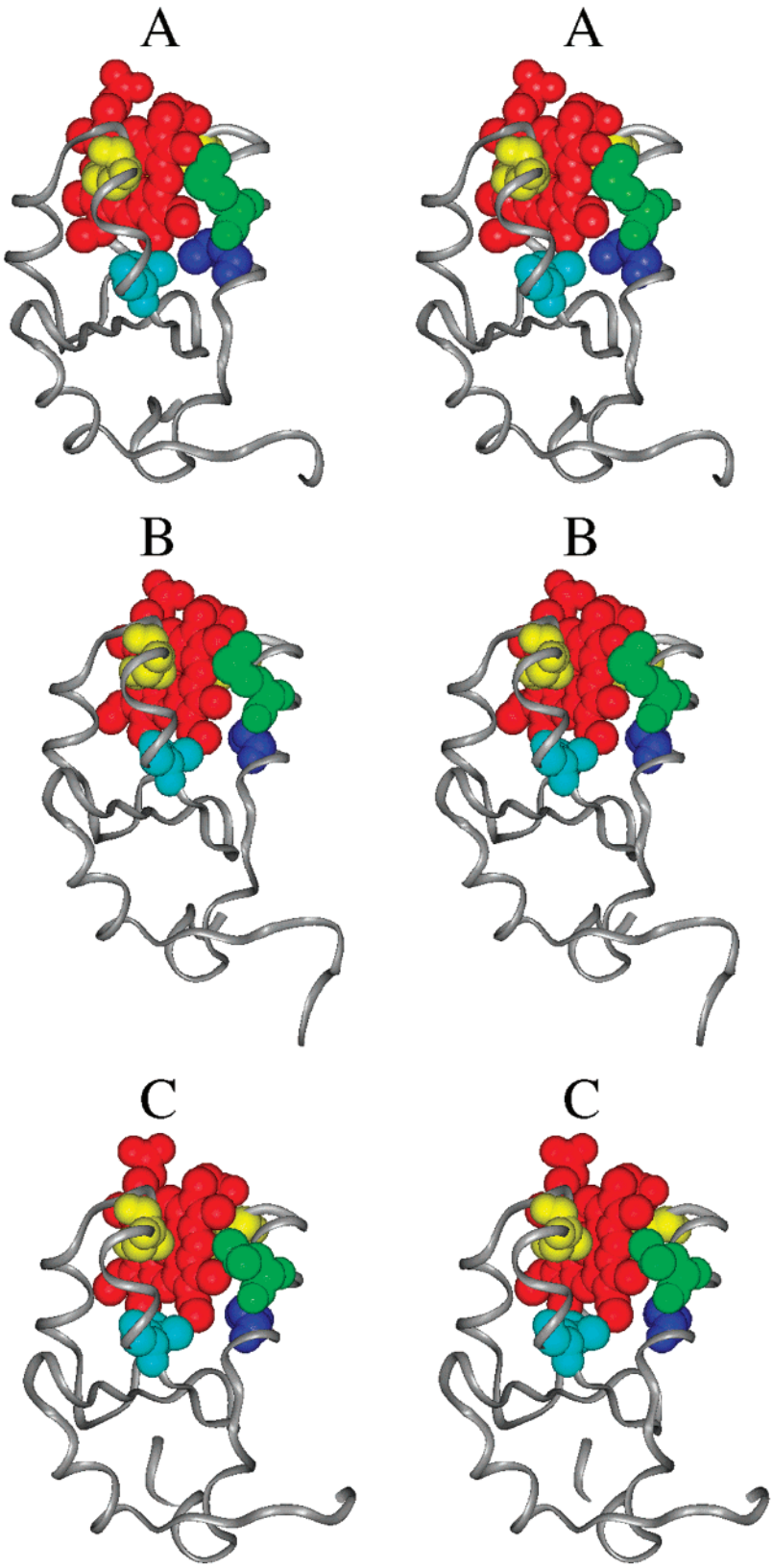

FIGURE 4: Stereo representations depicting key interactions among amino acid side chains and heme that are responsible for the ratio of hemin orientational isomers observed with the different mutants: (A) A18S/I32L/L47R triple mutant of rat OM cyt b_5; (B) A18S/I25L/I32L/L47R/L71S quintuple mutant of rat OM cyt b_5; (C) wild-type bovine Mc cyt b_5. In each structure heme is in red, residue 32 is in light blue, residue 71 is in blue, residue 70 is in green, and the heme axial ligands are in yellow.

group makes close contact with the methyl group on heme pyrrole ring II (isomer A), similar to the interaction between this heme methyl group and the side chain of Leu-23 in the bovine Mc protein. As a result, we consider it likely that the presence of Met-23 is one of the factors which favors isomer A in the rat OM quintuple mutant. Because the interactions between heme and the side chains of residue 23 in bovine Mc cyt b_5 and the rat OM quintuple mutant are so

```
                3         11          21          31          (A:B)
Rat OM Quint.   AVTYYRLE  EVAKRNTSEE  TWMVLHGRVY  DLTRFLSEHP (1.5:1)
Bovine Mc       AVKYYTLE  EIQKHNNSKS  TWLILHYKVY  DLTKFLEEHP (~9:1)
Human Mc        AVKYYTLE  EIQKHNHSKS  TWLILHHKVY  DLTKFLEEHP (~9:1)
Rat Mc          DVKYYTLE  EIQKHKDSKS  TWVILHHKVY  DLTKFLEEHP (1.6:1)

               41          51          61          71          81
Rat OM Quint.  GGEEVLREQA  GADATESFED  VGHSPDAREM  SKQYYIGDVH  PNDL
Bovine Mc      GGEEVLREQA  GGDATENFED  VGHSTDARELL SKTFIIGELH  PDDR
Human Mc       GGEEVLREQA  GGDATENFED  VGHSTDAREM  SKTFIIGELH  PDDR
Rat Mc         GGEEVLREQA  GGDATENFED  VGHSTDARELL SKTYIIGELH  PDDR
```

FIGURE 5: Amino acid sequence alignments of the heme-binding domains of the A18S/I25L/I32L/L47R/L71S quintuple mutant of rat OM cyt b_5 and of bovine, human, and rat Mc cyt b_5. The numbers in parentheses at the end of the first row indicate the equilibrium hemin isomer ratio for that protein. Residues considered most likely to contribute to the different hemin isomer ratios are underlined.

similar, it is not easy to predict the effect of replacing Met-23 in the quintuple mutant with Leu. Finally, the side chain of Leu-70 in the crystal structure of bovine Mc cyt b_5 is packed against the heme methyl group at position 1 (A 1Me; see Figure 4). The corresponding position in rat OM cyt b_5 is occupied by a Met. Because the side chain of Leu-70 is more restricted in its conformations than Met, it is more likely to experience unfavorable steric interactions if the A 1Me methyl group of hemin isomer A were to be replaced by the B 4V vinyl group of isomer B. We therefore predict that replacing Met-70 in the rat OM cyt b_5 quintuple mutant with Leu will increase the population of isomer A at the expense of isomer B. The roles of residues 23, 70, and 74 will be examined in more detail in future work.

Kinetics of Hemin Reorientation and Hemin Transfer. It is evident from the discussion above that, following polypeptide synthesis, hemin is incorporated into the apoprotein to form isomers A and B with essentially identical rates, thus leading to nascent protein exhibiting equimolar concentrations of both hemin orientational isomers. In the case of bovine Mc cyt b_5, the less stable isomer is gradually converted into the more stable isomer until equilibrium has been attained (*20*, *27*), as indicated in eq 3. This unimolecular

$$\mathrm{m} \underset{k_{-1}}{\overset{k_1}{\rightleftharpoons}} \mathrm{M} \qquad (3)$$

reaction, which is assumed to occur within a protein cage, has been shown to be the more likely mechanism for hemin reorientation in myoglobin (*24*, *29*) and in the bishistidine-coordinated hemoglobin from *Synechocystis* sp. (*41*). It is therefore reasonable to assume that the mechanism of hemin reorientation in cytochrome b_5 is also unimolecular (eq 3). Hence, at a given temperature the equilibrium constant for hemin isomer interconversion is defined by $K_{eq} = [\mathrm{M}]/[\mathrm{m}]$, where [M] and [m] represent the concentrations of the major and minor isomer, respectively. If the change in concentration of the major isomer as a function of time is given by eq 4, $[\mathrm{M}]_0$ and $[\mathrm{m}]_0$ are the concentrations of major and minor isomers at time zero and $[\mathrm{M}]_{eq}$ and $[\mathrm{m}]_{eq}$ represent the corresponding equilibrium concentrations, eqs 5 and 6 are readily obtained. A plot of the term $\ln\{([\mathrm{m}] - [\mathrm{m}]_{eq})/([\mathrm{m}]_0 - [\mathrm{m}]_{eq})\}$ vs time should be linear with slope $-(k_1 + k_{-1})$.

$$d[\mathrm{m}]/dt = -k_1[\mathrm{m}] + k_{-1}[\mathrm{M}] \qquad (4)$$

$$d[\mathrm{m}]/dt = (k_1 + k_{-1})([\mathrm{m}]_{eq} - [\mathrm{m}]) \qquad (5)$$

$$\ln\{([\mathrm{m}] - [\mathrm{m}]_{eq})/([\mathrm{m}]_0 - [\mathrm{m}]_{eq})\} = -(k_1 + k_{-1})t \qquad (6)$$

The equilibrium constant $K_{eq} = k_1/k_{-1}$ is obtained from the NMR spectrum when the isomer interconversion reaction has reached equilibrium. Values of k_1 listed in Table 2 were obtained from time-dependent NMR spectroscopic data analyzed using eq 6.

In a previous communication we reported that hemin reorientation is unmeasurably slow for wild-type rat OM cyt b_5 at pH 7.0 and 45 °C (*13*). However, disrupting the hydrophobic network encompassing residues Ala-18, Ile-32, Leu-36, and Leu-47 in the A18S/I32L/L47R triple mutant accelerated the rate of hemin reorientation and permitted its measurement; at pH 7.0 and 45 °C the triple mutant exhibits a half-life for hemin reorientation of 13.9 h (Table 2) (*13*). Interestingly, the point mutation L71S exerted a larger effect on the rate of hemin reorientation than did complete disruption of the originally identified hydrophobic patch (A18S/I32L/L47R), as is apparent from the k_1 measured for the L71S mutant which is nearly 2-fold larger than for the A18S/I32L/L47R triple mutant. Combining the L71S and A18S/I32L/L47R mutations produces a protein exhibiting a rate constant for hemin reorientation that is larger than that measured for either parent protein: the A18S/I32L/L47R/L71S quadruple mutant exhibits a k_1 ~5-fold larger than that of the triple mutant and ~2.5-fold larger than that of the L71S mutant. Incorporating the I25L mutation into the quadruple mutant increases k_1 by an additional factor of 1.2 with respect to the latter.

Of all the mutants of rat OM cyt b_5 examined in this study, only the A18S/I32L/L47R/L71S quadruple and A18S/I25L/I32L/L47R/L71S quintuple mutants are isolated with unequal concentrations of hemin isomers A and B (A:B ~ 1.2:1 in each case). The observation that partial hemin isomer equilibration occurs during expression of these mutants indicates that hemin is no longer kinetically trapped under physiological conditions. This observation prompted us to examine whether the hemin isomer ratio in freshly expressed and purified bovine Mc cyt b_5 corresponds to that observed at equilibrium (A:B ≈ 9:1). To this end, the gene coding for this protein was placed in the same expression vector used to obtain rat OM cyt b_5 (see Experimental Procedures), and the protein was expressed and purified using conditions identical to those employed for the rat OM mutants. As isolated, the hemin isomer ratio in the bovine Mc protein is A:B = 2.8:1, which is in agreement with the hypothesis that both hemin isomers are formed at the same rate, followed by reorientation of the minor isomer to achieve the equilibrium concentrations dictated by interactions between hemin and the polypeptide. In this context, it is interesting to

Table 3: Rate Constants for Hemin Transfer[a]

protein	pH 7.0 k_{-H} (h^{-1})	pH 5.0 $k_{-H,slow}$ (h^{-1})	pH 5.0 $k_{-H,fast}$ (h^{-1})
wild-type rat OM	*b*	~0.05[c]	
I25L	*b*	~0.08[c]	
A18S/I32L/L47R	*b*	≤0.27	≤1.5
L71S	*b*	0.26 ± 0.02	1.4 ± 0.2
A18S/I32L/L47R/L71S	~0.007[c]	2.5 ± 0.3	6.2 ± 0.4
A18S/I25L/I32L/L47R/L71S	~0.01[c]	8.3 ± 0.4	
bovine Mc tryptic fragment (this work)	0.28 ± 0.04	6.5 ± 0.5	
bovine Mc tryptic fragment (*24*)	0.23 ± 0.02	6.8 ± 0.5	

[a] Measured at 37 °C. [b] Too slow to measure. [c] Determined from initial rate data.

compare the rate of hemin reorientation exhibited by the A18S/I25L/I32L/L47R/L71S quintuple mutant, which is the fastest among the OM cyt b_5 proteins, with that exhibited by bovine Mc cyt b_5. Walker et al. reported that the half-life for reorientation of isomer B to isomer A at 24 °C is 12 h (*20*). By comparison, hemin in the quadruple and quintuple mutants of rat OM cyt b_5 is still kinetically trapped at 24 °C because ^{1}H NMR spectra acquired over a period of 29 h, more than 2-fold longer than the half-life for hemin reorientation in the Mc isoform, clearly show that the ratio of A and B isomers remains constant. Therefore, the rate of hemin reorientation in the quintuple mutant of rat OM cyt b_5 is still significantly slower than the rate of hemin reorientation exhibited by the bovine Mc isoform.

From the preceding discussion, it is apparent that disruption of both hydrophobic networks in the structure of rat OM cyt b_5 results in enhancement of the rate of hemin reorientation at 45 °C for all mutants except I25L. Hemin in the latter, as in wild-type OM cyt b_5, is kinetically trapped at this temperature. It was therefore of interest to investigate whether the mutations have similar effects on rates of hemin release. Rates of hemin release are typically obtained by measuring rate constants for hemin transfer from a heme donor protein to an appropriate apohemoprotein, which is present in excess (*33*, *42*). For the present studies we have used wild-type horse apoMb, as suitable changes in electronic absorption spectra accompany the hemin transfer reaction. The reactions are carried out in the presence of sucrose, which functions to stabilize the apoproteins (*33*). The rate constant for hemin transfer from the tryptic fragment of bovine Mc cyt b_5 to horse apoMb at pH 7 and 37 °C (k_{-H}) was determined in this manner from the fit of a plot relating the absorbance at 406 nm vs time to eq 7 , where A_t is the

$$A_t = A_\infty - \Delta A_{eq} \exp(-k_{-H} t) \quad (7)$$

absorbance at time *t*, A_∞ is the final absorbance, and ΔA_{eq} is the total change in absorbance. The value obtained is nearly identical to that determined by Mauk and co-workers using a mutant of horse apoMb as the receiving protein (Table 3) (*24*). In contrast, no transfer of hemin from rat OM cyt b_5 to apoMb is observed at the same pH and temperature, consistent with our previous conclusion that hemin is kinetically trapped under physiological conditions (in our previous reports, hemin transfer reactions were performed at 21 °C). Hemin in the L71S, I25L, and A18S/I32L/L47R mutants is also kinetically trapped at pH 7 and 37 °C. However, the A18S/I32L/L47R/L71S quadruple and A18S/I25L/I32L/L47R/L71S quintuple mutants exhibit observable hemin transfer under these conditions, albeit significantly slower than those exhibited by bovine Mc cyt b_5 (Table 3). Hence, upon complete disruption of the two hydrophobic patches in rat OM cyt b_5 hemin is no longer kinetically trapped under physiological conditions, as evidenced in both hemin reorientation and hemin transfer experiments. The fact that both processes are considerably slower than for bovine Mc cyt b_5 indicates that other, as yet unidentified, factors contribute to the remaining difference in kinetic barriers for these processes in the bovine Mc and rat OM proteins.

Hemin Release from Isomer A and from Isomer B Is Kinetically Resolved. Transfer of hemin from wild-type bovine Mc cyt b_5 to apoMb is approximately 30 times faster at pH 5.0 than at pH 7.0 (Table 3) (*24*). The faster rate at lower pH likely originates from the fact that the His ligands, once dissociated from iron, are more likely to become protonated before they bind iron again. In agreement with this expectation, lowering the pH to 5.0 at 37 °C facilitates hemin transfer from wild-type rat OM cyt b_5 to apoMb, but the reaction is still very slow ($t_{1/2} \approx 14$ h; Table 3). Whereas the conservative mutation of Ile-25 to Leu results in only a small acceleration, hemin transfer from the L71S and A18S/I32L/L47R mutants is considerably faster, reaching completion within about 16 h. For the A18S/I32L/L47R/L71S quadruple and A18S/I25L/I32L/L47R/L71S quintuple mutants, hemin transfer reactions are complete within approximately 90 and 30 min, respectively.

For the four rat OM cyt b_5 mutants exhibiting the fastest hemin transfer at pH 5.0, we were able to obtain rate constants by fitting plots relating the absorbance at 406 nm and time to eq 7. However, for the L71S, A18S/I32L/L47R, and A18S/I32L/L47R/L71S mutants, we found that fits of the data could be significantly improved if two first-order processes were considered (eq 8) rather than only one. For

$$A_t = A_\infty - \Delta A_{eq,fast} \exp(-k_{-H,fast} t) - \Delta A_{eq,slow} \exp(-k_{-H,slow} t) \quad (8)$$

example, when hemin transfer experiments were carried out with the L71S single mutant obtained immediately after expression and purification (A:B = 1:1), the plot relating time-dependent absorbance changes shown in Figure 6A was obtained. Fitting these data to the monoexponential eq 7 was less than optimum, as demonstrated by the relatively large residuals. Significantly improved results were obtained by fitting the data to the biexponential eq 8, as can be seen from the associated residual plot. Fitting the data to eq 8 yields two rate constants, $k_{-H,fast}$, describing a fast event, and $k_{-H,slow}$, describing a slow event. It is interesting that the ratio of these two constants, $k_{-H,slow}/k_{-H,fast} = 0.18$ (see Table 3), is nearly identical to the equilibrium hemin isomer ratio, A/B = 0.19 (see Table 2), obtained by NMR spectroscopy. Consequently, this finding suggests that the slow and fast phases originate from release of hemin from the more stable (A) and less stable (B) hemin orientational isomers, respectively. In agreement with this hypothesis, the slow ($\Delta A_{eq,slow}$) and fast ($\Delta A_{eq,fast}$) preexponential terms obtained from the fit of the data to eq 8 contribute almost equally to the overall kinetic

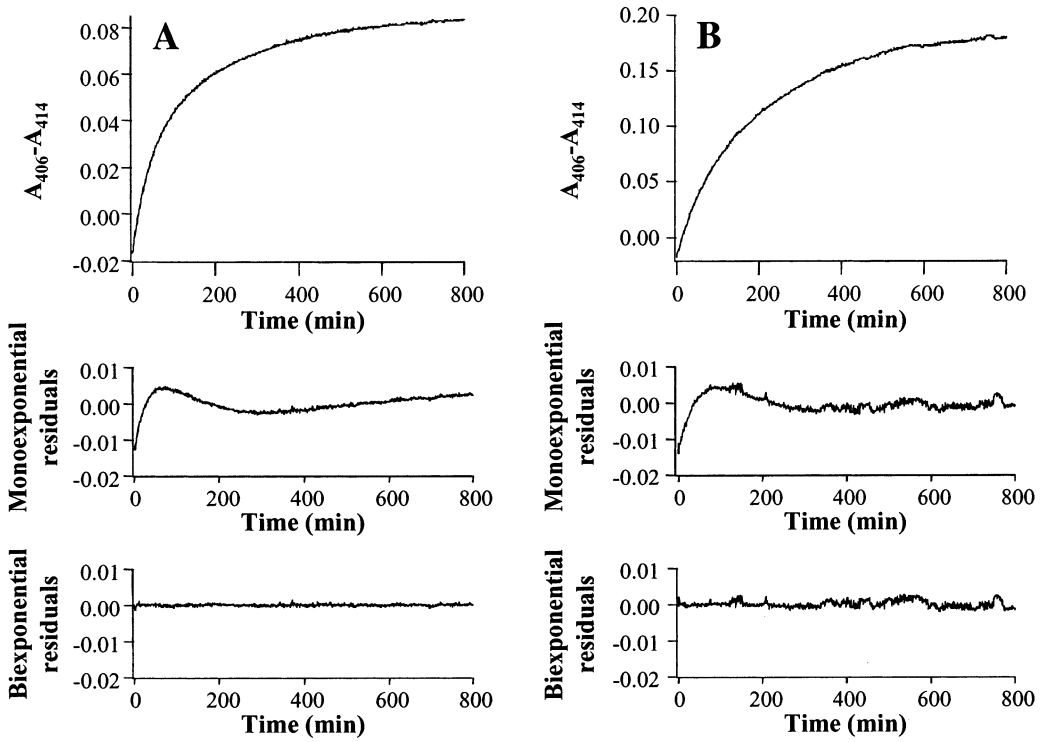

FIGURE 6: (A) Plot of absorbance vs time obtained from experiments where hemin is transferred from the L71S mutant of rat OM cyt b_5 to apoMb (top). The sample of the L71S mutant used in this experiment exhibited a 1:1 ratio of hemin isomers A and B. Residual plots are shown for fits of the data to eq 7 (middle) and to eq 8 (bottom). (B) Corresponding data obtained with a sample of the L71S mutant exhibiting a 5.2:1 ratio of hemin isomers A and B. Experiments were performed at 37 °C in 150 mM sodium acetate buffer, pH 5.0, containing 450 mM sucrose (*33*).

change ($\Delta A_{eq,slow}/\Delta A_{eq,fast} \sim 1.4/1$), as would be expected from the 1:1 ratio of hemin orientational isomers present in the sample. Additional evidence supporting the hypothesis that release of hemin from isomer A and isomer B can be kinetically resolved was obtained by studying the L71S mutant which had been previously incubated at 45 °C until the thermodynamically dictated equilibrium ratio, A:B = 5.2:1, had been attained. A plot relating the time-dependent absorbance changes observed during the course of this experiment is shown in Figure 6B. It is evident by simple inspection that hemin transfer is slower in the protein sample containing predominately isomer A (Figure 6B) than in the sample containing an equimolar mixture of isomer A and isomer B (Figure 6A). A monoexponential fit of the data (eq 7), again, is not optimum, as indicated by the associated residual plot, while use of the biexponential function (eq 8) results in an optimum fit. The two rate constants, $k_{-H,fast}$ and $k_{-H,\ slow}$, obtained from the biexponential fit are identical within error to those obtained with the protein sample exhibiting a 1:1 ratio of hemin isomers. Consequently, the slower overall rate of hemin transfer must arise from the fact that the kinetic term, $\Delta A_{eq,slow}$, corresponding to the more stable isomer (isomer A) contributes more to the overall kinetic change than does the kinetic term, $\Delta A_{eq,fast}$, corresponding to the less stable isomer (isomer B). The values obtained from the fitting process indicate that, indeed, the relative contributions of the two preexponential terms in eq 8, $\Delta A_{eq,slow}/\Delta A_{eq,fast} \sim 5.6/1$, closely match the ratio of the more stable and less stable isomers (A/B = 5.2/1), thus corroborating the idea that hemin transfer data must be fit to a biexponential function because transfer from the more stable isomer is slower than transfer from the less stable isomer. Similar results were obtained for the A18S/I32L/L47R and A18S/I32L/L47R/L71S mutants. On the other hand, fits of hemin transfer data for the A18S/I25L/I32L/L47R/L71S quintuple mutant were not significantly improved by using a double exponential function, a finding that is consistent with the smaller difference in hemin orientational isomers at equilibrium for this mutant.

Release of hemin from the α and β subunits of human hemoglobin has similarly been kinetically resolved by electronic absorption spectroscopy (*33*). However, our results represent the first case where the release of two hemin orientational isomers has been kinetically resolved. The fact that release of hemin orientational isomers A and B of these cyt b_5 mutants can be kinetically resolved at pH 5.0 indicates that rebinding of hemin by the cyt b_5 mutant following its release is much slower than binding of the released hemin by apoMb. In other words, hemin transfer is clearly faster than hemin reorientation at pH 5.0.

Despite the fact that only a 10-fold excess of apoMb could be employed in the hemin transfer reactions with the L71S and A18S/I32L/L47R mutants at pH 5.0 and 37 °C, the electronic absorption spectra recorded at the end of the reactions are essentially identical to the spectrum of horse Mb. Furthermore, when the ratio of apoMb to L71S cyt b_5 was decreased from 10:1 to 5:1, there was no observed change in the fitted rate constants. Both of these findings suggest that transfer of hemin from the L71S mutant to horse apoMb reaches completion in the presence of a 10-fold excess of horse apomyoglobin. In contrast, a measurable change in the fitted rate constants was observed for the A18S/I32L/L47R triple mutant upon a similar change in ratio of apoMb to cyt b_5. For this mutant, therefore, we cannot rule

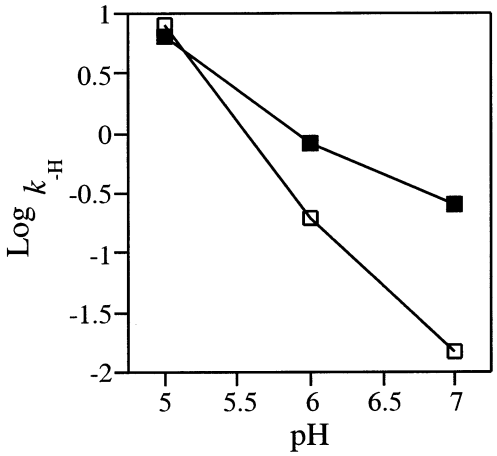

FIGURE 7: Plots of k_{-H} as a function of pH obtained for the tryptic fragment of bovine Mc cyt b_5 (■) and the A18S/I25L/I32L/L47R/L71S quintuple mutant of rat OM cyt b_5 (□).

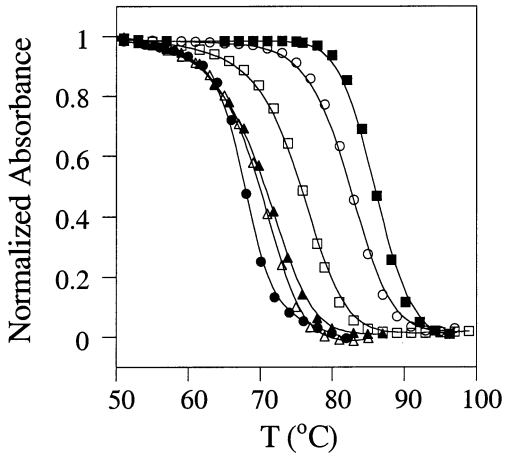

FIGURE 8: Plots of normalized absorbance at 412 nm (Soret band λ_{max}) vs temperature for wild-type rat OM cyt b_5 (●), the tryptic fragment of wild-type bovine Mc cyt b_5 (■), and the A18S/I32L/L47 (○), L71S (△), A18S/I32L/L47R/L71S (▲), and A18S/I25L/I32L/L47R/L71S (□) mutants of rat OM cyt b_5. Data were acquired in 50 mM potassium phosphate buffer, pH 7.0.

out the possibility that the rate constants obtained when using a 10-fold excess of horse apoMb include some contribution from transfer of hemin from Mb back to apocyt b_5. Therefore, we represent the hemin transfer rate constants for the A18S/I32L/L47R in Table 3 as upper limits. Because in the present work we are primarily interested in the relative propensities toward hemin loss among various rat OM cyt b_5 mutants and how these compare to wild-type bovine Mc cyt b_5, we have opted to refrain from a detailed kinetic analysis that would take return hemin transfer into account for this mutant.

Summarizing the data in Table 3, we find that hemin transfer rate constants for the major and minor isomers of the L71S and A18S/I32L/L47R mutants at pH 5.0 and 37 °C are similar. However, combining these mutations in the A18S/I32L/L47R/L71S quadruple mutant leads to increases in hemin transfer rate constants of ∼10-fold and ∼5-fold for the major (slow) and minor (fast) isomers, respectively. The major isomer of this mutant loses hemin at slightly less than half the rate observed for wild-type bovine Mc cyt b_5 at pH 5. Finally, the A18S/I25L/I32L/L47R/L71S quintuple mutant transfers heme at pH 5 at a rate faster than that observed for bovine Mc cyt b_5 under identical conditions. These observations stand in sharp contrast to the behavior of these proteins at pH 7.0, where the quintuple mutant transfers heme more than 30-fold slower than the bovine Mc protein. To examine the pH dependence of the reaction in more detail, we compared hemin transfer rate constants for the A18S/I25L/I32L/L47R/L71S quintuple mutant of rat OM cyt b_5 and for the wild-type bovine Mc protein measured at pH 5.0, 6.0, and 7.0 (Figure 7). At pH 5.0, bovine Mc cyt b_5 and the rat OM quintuple mutant release hemin with nearly identical rates. However, the rate of hemin transfer for the bovine Mc protein decreases by a factor of ∼30 between pH 5.0 and pH 7.0, an observation that is in agreement with the results recently reported by Mauk and co-workers (*24*). In contrast, over the same pH range, the hemin transfer rate constant for the rat OM quintuple mutant decreases by a factor of approximately 830. These observations suggest that at least one of the histidine axial ligands in Mc cyt b_5 is protonated more readily than its counterpart(s) in rat OM cyt b_5 as pH is decreased, thereby leading to faster rates of hemin release and hemin reorientation. In future studies we hope to identify the factors responsible for the markedly different effects of pH on hemin release for these proteins, as well as to explain the mechanism responsible for the observed results.

Thermal Denaturation Studies. An additional feature that distinguishes rat OM cyt b_5 from the Mc isoforms is its significantly greater stability toward thermal denaturation (Figure 8, Table 4); the temperature at which rat OM cyt b_5 is 50% denatured (its T_m value) is nearly 20 °C higher than for the bovine Mc isoform (*13*). Thermal denaturation of cyt b_5 is accompanied by disruption of the bonds between hemin and the protein, which we monitor by changes in electronic absorption spectra (the Soret band λ_{max} shifts from 412 nm in the folded protein to 390 nm in the denatured protein). As is commonly observed in thermal denaturation studies of cytochromes b_5 (*43*, *44*), electronic absorption spectra recorded as a function of temperature exhibit isosbestic behavior.

Such an observation is consistent with the two-state unfolding equilibrium represented in eq 9, where folded holoprotein (F·H) is in equilibrium with unfolded apoprotein (U) and free hemin (H). Such a scenario, however, contradicts the well-known hydrophobicity of hemin, which causes it to aggregate (*45*) or to interact preferentially with other hydrophobic species (*46*−*48*) when in aqueous solution. In fact, studies with cyt b_{562} have demonstrated that hemin forms a relatively stable complex with the unfolded apoprotein and that this complex is partially populated even at elevated temperatures (*51*). Hence, thermal denaturation of cyt b_{562} is best described by the three-state equilibrium in eq 10, where U·H is the complex between hemin and the unfolded apoprotein (*51*), even though electronic absorption spectra of cyt b_{562} recorded as a function of temperature exhibit isosbestic behavior (*52*). Consequently, we cannot discount the possibility that eq 10 also describes the thermal denaturation of cyt b_5.

$$\mathrm{F{\cdot}H} \rightleftarrows \mathrm{U} + \mathrm{H} \tag{9}$$

$$\mathrm{F{\cdot}H} \rightleftarrows \mathrm{U{\cdot}H} \rightleftarrows \mathrm{U} + \mathrm{H} \tag{10}$$

The data in Table 4 show that values of T_m determined for rat OM cyt b_5 and its mutants vary over a range of about

Table 4: Thermal and Chemical Denaturation Data

	holoproteins[a]		apoproteins[b]		
	T_m (°C)	C_m (M)	C_m (M)	m (kcal mol^{-1} M^{-1})	ΔG^{H_2O} (kcal/mol)
wild-type rat OM	85.5 ± 0.5	2.04 ± 0.08	1.31 ± 0.02	2.4 ± 0.2	3.2 ± 0.1
I25L	84.7 ± 0.3	1.91 ± 0.03	*c*	*c*	*c*
A18S/I32L/L47R	81.2 ± 1.0	1.71 ± 0.02	1.13 ± 0.02	2.6 ± 0.2	2.9 ± 0.1
L71S	75.3 ± 0.4	1.40 ± 0.02	~0.3	*c*	~0.8[d]
A18S/I32L/L47R/L71S	71.1 ± 0.9	1.13 ± 0.03	*c*	*c*	*c*
A18S/I25L/I32L/L47R/L71S	69.0 ± 0.9	0.97 ± 0.02	*c*	*c*	*c*
bovine Mc tryptic (this work)	67.6 ± 0.3	1.52 ± 0.02	1.63 ± 0.04	1.7 ± 0.2	2.7 ± 0.2
bovine Mc (lit.)	67.4 ± 0.7[e]		~1.6[f]	1.9 ± 0.4[f]	2.8 ± 0.4[f]

[a] GdmSCN used in chemical denaturation studies at 25 °C. [b] GdmCl used in chemical denaturation studies at 25 °C. [c] Not determined. [d] Calculated by multiplying the approximate C_m value by the average m values for the wild-type and A18S/I32L/L47R mutant proteins (see eq 2). [e] Determined for the tryptic fragment (*49*). [f] Determined using a variant of bovine Mc apocyt b_5 containing 104 residues (*50*).

16 °C. As expected, the conservative replacement of Ile-25 with Leu causes only a minor decrease in T_m, from 85.5 to 84.7 °C, whereas the single point mutation L71S (T_m = 75.3 °C) exerts a greater effect than does complete disruption of the originally identified hydrophobic patch in the A18S/I32L/L47R triple mutant (T_m = 81.2 °C). Further destabilization is effected by combining the L71S and A18S/I32L/L47R mutations as evidenced by the T_m value for the A18S/I32L/L47R/L71S quadruple mutant (71.1 °C), which is lower than the T_m values exhibited by either of the parent proteins. Finally, introducing the I25L mutation into the quadruple mutant yields an A18S/I25L/I32L/L47R/L71S quintuple mutant exhibiting a T_m value of 69.9 °C, only 1.5 °C higher than that of the bovine protein.

A characteristic of cytochromes b_5 (*43*, *53*), also observed in our thermal denaturation experiments, is that typically less than 60% of the protein refolds after cooling a fully denatured sample back to 25 °C. Furthermore, the extent of refolding decreases proportionately to the time the sample is heated above its T_m. Thus, because the thermal denaturation reactions are not fully reversible and it is not clear whether the unfolding reaction conforms to a two-state (eq 9) or a three-state (eq 10) equilibrium, we chose not to extract thermodynamic parameters from the thermal denaturation data until we have examined the mechanism of the reaction in greater detail. However, inspection of Figure 8 reveals that the slopes of the unfolding transition regions for wild-type rat OM cyt b_5 and its mutants are similar, indicating that decreases in T_m for those proteins are reasonable indicators of relative thermodynamic stability. In contrast, the slope of the unfolding transition region for bovine Mc cyt b_5 is markedly sharper, indicating that it may be more stable than its T_m value suggests. In fact, results of chemical denaturation studies described in the following section strongly suggest that bovine Mc cyt b_5 is actually more stable than the rat OM cyt b_5 quintuple mutant.

Chemical Denaturation Studies. Treatment of cyt b_5 with denaturants such as guanidinium chloride (GdmCl) is also conducive to protein unfolding (*30*). As in thermal denaturation studies, disruption of bonds between the His ligands and hemin can be monitored by following changes in electronic absorption spectra. Changes in protein structure indicating protein unfolding can be examined independently by fluorescence spectroscopy, which monitors the change in environment of the invariant residue Trp-22. The latter resides in a region of the protein whose structure is not significantly perturbed by loss of hemin under nondenaturing conditions (*54*, *55*). This region, defined as core 1, includes the β-sheet which comprises the base of the heme-binding pocket. In contrast, the structure of the four-helix bundle which surrounds the heme (core 2) is disrupted upon loss of heme in nondenaturing conditions (*54*, *55*). Previous chemical denaturation studies with wild-type bovine Mc and rat OM cyt b_5 using electronic absorption and fluorescence spectroscopy have shown that protein unfolding and disruption of the Fe(III)−His bonds are coupled events under denaturing conditions (*23*). Further experiments revealed a decrease in stability for the A18S/I32L/L47R mutant without uncoupling these events (*13*), a relationship that is maintained in the A18S/I25L/I32L/L47R/L71S quintuple mutant, the least stable mutant of rat OM cyt b_5 examined in this study (data not shown).

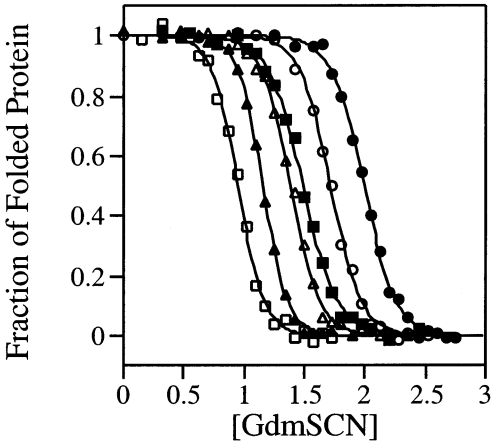

FIGURE 9: Data from GdmSCN-mediated chemical denaturation of wild-type rat OM cyt b_5 (●), the tryptic fragment of wild-type bovine Mc cyt b_5 (■), and the A18S/I32L/L47 (○), L71S (△), A18S/I32L/L47R/L71S (▲), and A18S/I25L/I32L/L47R/L71S (□) mutants of rat OM cyt b_5. All measurements were performed at 25 °C in 30 mM MOPS buffer, pH 7.0.

Chemical denaturation studies of the proteins noted above required several hours of incubation with GdmCl before reproducible denaturation curves could be obtained (*13*). Because the more potent denaturant guanidinium thiocyanate (GdmSCN) (*56*) enabled us to obtain reproducible denaturation curves with incubation times of 1 h (Figure 9), it was used for the chemical denaturation studies described herein. Spectra recorded as a function of [GdmSCN] monitored by electronic absorption spectroscopy revealed the expected shift of the heme Soret band from 412 to 390 nm, although deviation from isosbestic behavior was observed. The deviation became more pronounced as the concentration of

GdmSCN surpassed the amount needed to fully unfold the protein as determined by the absence of further decreases in absorbance at 412 nm. To examine this situation further, we performed refolding experiments with wild-type rat OM cyt b_5 and the A18S/I32L/L47R/L71S quadruple mutant. Each protein was incubated for 1 h in a solution containing the minimum concentration of GdmSCN needed to cause complete denaturation (2.5 M for rat OM cyt b_5; 1.5 M for the quadruple mutant) and then was diluted to nondenaturing conditions. Whereas ≥95% of the quadruple mutant refolded upon dilution, less than 60% refolding was observed for the wild-type protein. A sample of the quadruple mutant denatured with 2.5 M GdmSCN also exhibited less than 60% refolding upon return to native conditions. These results suggest that hemin remains associated with the unfolded protein at low denaturant concentrations, which is favorable for refolding, but is released at higher [GdmSCN], resulting in hemin aggregation upon dilution, which is not conducive to refolding. Similar findings have been recently reported for Mb denatured with GdmCl (*57*), thus providing support to our hypothesis. Consequently, the chemical denaturation reactions are probably best described by the three-state equilibrium in eq 10. Studies aimed at better understanding the mechanism of cyt b_5 unfolding in chemical denaturation experiments are presently underway in our laboratories.

Because the mechanism of GdmSCN-mediated chemical denaturation has not yet been firmly established and may in fact differ across the range of proteins examined, we report herein only the concentration of GdmSCN at which each protein is 50% unfolded (C_m values in Table 4). Differences in C_m values among various mutants of a protein are generally considered to be good indicators of relative thermodynamic stability (*58*). Hence, the chemical denaturation data indicate that the thermodynamic stability of rat OM cyt b_5 and its mutants decreases in the order wild type > I25L > A18S/I32L/L47R > L71S > A18S/I32L/L47R/L71S > A18S/I25L/I32L/L47R/L71S, identical to the order indicated in thermal denaturation studies. The results of these experiments clearly show that replacing the residues comprising the two hydrophobic clusters in rat OM cyt b_5 with the corresponding residues in the bovine Mc protein results in significant destabilization of the protein. However, the data also yield the surprising result that the quintuple mutant of rat OM cyt b_5 is less stable than the bovine Mc isoform, the protein which served as the template for its creation. Other, as yet unidentified, differences in structure between the two proteins clearly exert compensating effects.

To better understand the results of chemical denaturation experiments with the holoproteins, we investigated the stability of the corresponding apoproteins. GdmCl was used as the denaturant in these studies, and protein unfolding was monitored by fluorescence spectroscopy, which indicates changes in the environment of the invariant residue Trp-22. Plots relating the fraction of folded apoprotein vs [GdmCl] for the proteins examined in this study are shown in Figure 10. Comparing the results for the wild-type rat OM and bovine Mc apoproteins, we find that the denaturation curves in each case fit very well to eq 1 (Figure 10), indicating that unfolding in each case is cooperative and involves no observable intermediates. Furthermore, fully denatured wild-type rat OM and bovine Mc apocyt b_5 each exhibit greater than 95% refolding upon dilution to native conditions as determined by fluorescence spectroscopy, demonstrating that the unfolding reactions are reversible. The denaturation data we obtained for the bovine Mc apoprotein are nearly identical to results reported by Manyusa and Whitford for a longer variant of the bovine Mc apoprotein (*50*). Interestingly, the C_m value for bovine Mc apocyt b_5 is greater than that of the rat OM apoprotein, despite being slightly less stable (Table 4). The reason for this apparent discrepancy is that the transition from native to denatured protein occurs over a wider range of GdmCl concentrations for bovine Mc apocyt b_5 than for the wild-type rat OM apoprotein, thus leading to a significantly smaller value of *m*.

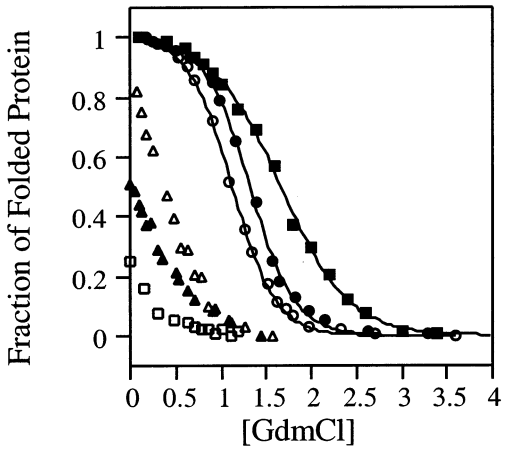

FIGURE 10: Data from GdmCl-mediated chemical denaturation of wild-type rat OM apocyt b_5 (●), the tryptic fragment of wild-type bovine Mc apocyt b_5 (■), and the A18S/I32L/L47 (○), L71S (△), A18S/I32L/L47R/L71S (▲), and A18S/I25L/I32L/L47R/L71S (□) mutants of rat OM apocyt b_5. All measurements were performed at 25 °C in 30 mM MOPS buffer, pH 7.0. The lines through the data points for the first three proteins represent the best fit of the data to eq 1. The fraction folded indicated for the last three proteins is estimated on the basis of the overall change in fluorescence intensity upon complete unfolding of those proteins compared to the values obtained for wild-type rat OM cyt b_5 and the A18S/I32L/L47R triple mutant.

It is important to note that well-defined native baselines were not obtained for either wild-type protein, and for this reason we believe that it is best to regard the data reported for them in Table 4 as estimates. Furthermore, additional experimentation is required in order to firmly establish whether the unfolding reactions for these apoproteins are described by two-state equilibria. However, results reported for rat (*59*) and rabbit (*60*) Mc apocytochromes b_5 suggest that such a scenario is likely. These and other issues relating to the stability of the rat OM and bovine Mc apoproteins will be the focus of future studies.

Disruption of the originally identified hydrophobic cluster in rat OM cyt b_5 by way of the A18S/I32L/L47R triple mutant causes essentially no change in apoprotein stability relative to the wild-type apoprotein. In stark contrast, the L71S mutant apoprotein is not fully folded in water, as evidenced by the complete absence of a plateau region at low denaturant concentrations in the plot of fluorescence intensity vs [GdmCl] (Figure 10). Further evidence is provided by the fact that the change in fluorescence emission intensity upon complete denaturation of the L71S apoprotein is approximately 80% of that observed for the wild-type and triple mutant apoproteins, indicating that the protein is about 20% denatured in aqueous solution. Plateau regions at low

denaturant concentration are also absent for the A18S/I32L/L47R/L71S quadruple and A18S/I25L/I32L/L47R/L71S quintuple mutant apoproteins (Figure 10). Changes in fluorescence intensity upon complete denaturation for these mutant apoproteins are even smaller than for the L71S mutant (50% and 25%, respectively, relative to the magnitude observed for the wild-type and triple mutant apoproteins), suggesting that they are even less stable.

On the basis of the results described above, it is evident that the two hydrophobic clusters in rat OM cyt b_5 play key roles in stabilizing its fold both in the presence and in the absence of heme, with Leu-71 being of particular importance. We surmise that Leu-71 performs its stabilizing roles in the apo- and holoproteins in the same way, namely, through hydrophobic interactions. In the apoprotein, these would include interactions with the side chains of Phe-58 and Ile-25. The substantially diminished stabilities of the rat OM cyt b_5 apoproteins containing Ser-71 relative to the wild-type apoprotein are nonetheless puzzling, considering that (1) the wild-type rat OM and bovine Mc apoproteins exhibit similar thermodynamic stabilities (Table 4) and (2) bovine Mc apocyt b_5 contains the residues that have been introduced into the rat OM protein. On the basis of these considerations, we can conclude that stabilization of bovine Mc apocyt b_5 derives from an alternate set of interactions between amino acid side chains.

Concluding Remarks. The mutants of rat OM cyt b_5 that have been discussed in this paper were generated with the intention of replacing two distinct hydrophobic clusters with the corresponding regions of mammalian Mc cytochromes b_5. This is part of a larger effort aimed at engineering the stability and hemin-binding properties of bovine Mc cyt b_5 into rat OM cyt b_5 to identify the structural factors responsible for the remarkable differences between the two proteins. As demonstrated in our discussion of the X-ray crystal structure of the quintuple mutant, in which replacement of the hydrophobic clusters is complete, we have been successful in introducing the desired structural elements. We conducted this investigation under the assumption that the hydrophobic clusters contribute to the greater stability of the rat OM protein and that they might also be responsible for the higher kinetic barriers for hemin release and hemin reorientation. The results of our hemin transfer, hemin reorientation, and protein stability studies support these predictions. In fact, comparing the data in Tables 2−4 indicates that decreases in protein stability correlate rather well with increasing rates of hemin transfer and hemin reorientation attained upon gradual disruption of the two hydrophobic networks in the rat OM protein. It is intriguing, however, that the rat OM quintuple mutant, although less stable than bovine Mc cyt b_5, exhibits considerably slower rates of hemin transfer and hemin reorientation at pH 7.0. Additional factors clearly contribute to the remaining differences in biophysical properties that distinguish the quintuple mutant from the bovine Mc protein. This is further illustrated by the observation that the quintuple mutant apoprotein and all other mutant apoproteins containing Ser at position 71 are much less stable than bovine Mc apocyt b_5, even though wild-type rat OM and bovine Mc apocyt b_5 exhibit similar stabilities as determined in chemical denaturation experiments. This finding has highlighted the unexpectedly critical role of Leu-71 in stabilizing the fold of rat OM cyt b_5 in the absence of heme, a role that likely involves key hydrophobic interactions with the side chains of Phe-58 and Ile-25. The absence of corresponding interactions in bovine Mc apocyt b_5 and other mammalian Mc apocytochromes b_5, which contain Ser at position 71, indicates that stabilization of their folds must be accomplished by alternative means. Hence, in addition to aiding us in better understanding the properties of rat OM cyt b_5, the studies described herein have revealed yet another critical difference between this protein and the mammalian Mc isoforms.

ACKNOWLEDGMENT

We thank Prof. Grant Mauk for providing us with the pUC19 plasmid harboring the gene for the tryptic fragment of bovine Mc cyt b_5 and Profs. Mark Hargrove and Richard Schowen for helpful discussions regarding hemin transfer experiments. Funds for the Oklahoma Statewide Shared NMR Facility were provided by the National Science Foundation (Grant BIR-952269), The Oklahoma State Regents for Higher Education, the W. M. Keck Foundation, and Conoco, Inc.

REFERENCES

1. Kuroda, R., Ikenoue, T., Honsho, M., Tsujimoto, S., Mitoma, J., and Ito, A. (1998) *J. Biol. Chem. 273*, 31097−31102.
2. Lederer, F., Ghrir, R., Guiard, B., Cortial, S., and Ito, A. (1983) *Eur. J. Biochem. 132*, 95−102.
3. Fukushima, K., and Sato, R. (1973) *J. Biochem. 74*, 161−173.
4. Rivera, M., Barillas-Mury, C., Christensen, K. A., Little, J. W., Wells, M. A., and Walker, F. A. (1992) *Biochemistry 31*, 12233−12240.
5. Mathews, F. S., Gerwinsky, E. W., and Argos, P. (1979) in *The Porphyrins* (Dolphin, D., Ed.) pp 107−147, Academic Press, New York.
6. Cristiano, R. J., and Steggles, A. W. (1989) *Nucleic Acids Res. 17*, 799.
7. Strittmatter, P., and Ozols, J. (1966) *J. Biol. Chem. 241*, 4787−4792.
8. Dariush, N., Fisher, C. W., and Steggles, A. W. (1988) *Protein Sequences Data Anal. 1*, 351−353.
9. VanDerMark, P. K., and Steggles, A. W. (1997) *Biochem. Biophys. Res. Commun. 240*, 80−83.
10. Yoo, M., and Steggles, A. W. (1988) *Biochem. Biophys. Res. Commun. 156*, 576−580.
11. Mitoma, J., and Ito, A. (1992) *EMBO J. 11*, 4197−4203.
12. Marra, M., Hillier, L., Allen, M., Bowles, M., Dietrich, N., Dubuquet, T., Geisel, S., Kucaba, T., Lacy, M., Le, M., Martin, J., Morris, M., Schellenberg, K., Steptoe, M., Tan, F., Underwood, K., Moore, B., Theising, B., Wylie, T., Lennon, G., Soares, B., Wilson, R., and Waterston, R. (1996) Direct submission to the EMBL/GenBank/DDBJ Databases (accession code P56395).
13. Altuve, A., Silchenko, S., Lee, K.-H., Kuczera, K., Terzyan, S., Zhang, X., Benson, D. R., and Rivera, M. (2001) *Biochemistry 40*, 9469−9483.
14. Durley, R. C. E., and Mathews, F. S. (1996) *Acta Crystallogr. D52*, 65−76.
15. Rodriguez-Maranon, M. J., Qiu, F., Stark, R. E., White, S. P., Zhang, X., Foundling, S. I., Rodriguez, V., Schilling, C. L., III, Bunce, R. A., and Rivera, M. (1996) *Biochemistry 35*, 16378−16390.
16. Rivera, M., Wells, M. A., and Walker, F. A. (1994) *Biochemistry 33*, 2161−2170.
17. Rivera, M., Seetharaman, R., Girdhar, D., Wirtz, M., Zhang, X., Wang, X., and White, S. (1998) *Biochemistry 37*, 1485−1494.
18. Wirtz, M., Oganesyan, V., Zhang, X., Studer, J., and Rivera, M. (2000) *Faraday Discuss. 116*, 221−234.
19. Reid, L. S., Taniguchi, V. T., Gray, H. B., and Mauk, A. G. (1982) *J. Am. Chem. Soc. 104*, 7516−7519.
20. Walker, F. A., Emrick, D., Rivera, J. E., Hanquet, B. J., and Buttlaire, D. H. (1988) *J. Am. Chem. Soc. 110*, 6234−6240.

21. Mauk, A. G., Mauk, M. R., Moore, G. R., and Northrup, S. (1995) *J. Bioenerg. Biomembr. 27*, 311−330.
22. Rodgers, K. K., and Sligar, S. G. (1991) *J. Am. Chem. Soc. 113*, 9419−9421.
23. Silchenko, S., Sippel, M. L., Kuchment, O., Benson, D. R., Mauk, A. G., Altuve, A., and Rivera, M. (2000) *Biochem. Biophys. Res. Commun. 271*, 467−472.
24. Hunter, C. L., Lloyd, E., Eltis, L. D., Rafferty, S. P., Lee, H., Smith, M., and Mauk, A. G. (1997) *Biochemistry 36*, 1010−1017.
25. La Mar, G. N., Burns, P. D., Jackson, J. T., Smith, K. M., Langry, K. C., and Strittmatter, P. (1981) *J. Biol. Chem. 256*, 6075−6079.
26. Lee, K.-B., Jun, E., La Mar, G. N., Rezzano, I. N., Pandey, R. K., Smith, K. M., Walker, F. A., and Buttlaire, D. H. (1991) *J. Am. Chem. Soc. 113*, 3576−3583.
27. McLachlan, S. J., La Mar, G. N., Burns, P. D., Smith, K. M., and Langry, K. C. (1986) *Biochim. Biophys. Acta 874*, 274−284.
28. Funk, W. D., Lo, T. P., Mauk, M. R., Brayer, G. D., MacGillivray, R. T. A., and Mauk, A. G. (1990) *Biochemistry 29*, 5500−5508.
29. La Mar, G. N., Toi, H., and Krishnamoorthi, R. (1984) *J. Am. Chem. Soc. 106*, 6395−6401.
30. Pace, N. C. (1986) *Methods Enzymol. 131*, 267−280.
31. Greene, R. F., and Pace, C. N. (1974) *J. Biol. Chem. 249*, 5388−5393.
32. Teale, F. W. J. (1959) *Biochim. Biophys. Acta 35*, 453.
33. Hargrove, M. S., Singleton, E. W., Quillin, M. L., Ortiz, L. A., Phillips, G. N., Jr., Olson, J. S., and Mathews, A. J. (1994) *J. Biol. Chem. 269*, 4207−4214.
34. Harrison, S. C., and Blout, E. R. (1965) *J. Biol. Chem. 240*, 299−303.
35. Brunger, A. T., Adams, P. D., Clore, G. M., De Lano, W. L., Gros, P., Grosse-Kunstleve, R. W., Jiang, J. S., Kuszewski, J., Nilges, M., and Pannu, N. S. (1998) *Acta Crystallogr. D54*, 905−921.
36. Roussel, A., and Cambillau, C. (1989) in *Silicon Graphics Geometry Partners Directory*, pp 77−79, Silicon Graphics, Mountain View, CA.
37. Lloyd, E., Ferrer, J. C., Funk, W. D., Mauk, M. R., and Mauk, A. G. (1994) *Biochemistry 33*, 11432−11437.
38. Mortuza, G. B., and Whitford, D. (1997) *FEBS Lett. 412*, 610−614.
39. Banci, L., Bertini, I., Rosato, A., and Scacchieri, S. (2000) *Eur. J. Biochem. 267*, 755−766.
40. Pochapsky, T. C., Sligar, S. G., McLachlan, S. J., and La Mar, G. N. (1990) *J. Am. Chem. Soc. 112*, 5258−5263.
41. Lecomte, J. T. J., Scott, N. L., Vu, B. C., and Falzone, C. J. (2001) *Biochemistry 40*, 6541−6552.
42. Smith, M. L., Paul, J., Ohlsson, P. I., Hjortsberg, K., and Paul, K. G. (1991) *Proc. Natl. Acad. Sci. U.S.A. 88*, 882−886.
43. Kitagawa, T., Sugiyama, T., and Yamano, T. (1982) *Biochemistry 21*, 1680−1686.
44. Xue, L.-L., Wang, Y.-H., Xie, Y., Yao, P., Wang, W.-H., Qian, W., Huang, Z.-X., Wu, J., and Xia, Z.-X. (1999) *Biochemistry 38*, 11961−11972.
45. White, W. I. (1978) in *The Porphyrins* (Dolphin, D., Ed.) Chapter 7, Academic Press, New York.
46. Simplicio, J., Schwenzer, K., and Maenpa, F. (1975) *J. Am. Chem. Soc. 97*, 7319−7326.
47. Mazumdar, S., and Mitra, S. (1993) *Struct. Bonding 81*, 115−145.
48. Wardell, M., Wang, Z., Ho, J. X., Robert, J., Ruker, F., Ruble, J., and Carter, D. C. (2002) *Biochem. Biophys. Res. Commun. 291*, 813−819.
49. Hewson, R., Newbold, R. J., and Whitford, D. (1993) *Protein Eng. 6*, 953−964.
50. Manyusa, S., and Whitford, D. (1999) *Biochemistry 38*, 9533−9540.
51. Robinson, C. R., Liu, Y., Thomson, J. A., Sturtevant, J. M., and Sligar, S. G. (1997) *Biochemistry 36*, 16141−16146.
52. Fisher, M. T. (1991) *Biochemistry 30*, 10012−10018.
53. Newbold, R. J., Hewson, R., and Whitford, D. (1992) *FEBS Lett. 314*, 419−424.
54. Moore, C. D., and Lecomte, J. T. J. (1993) *Biochemistry 32*, 199−207.
55. Storch, E. M., and Daggett, V. (1996) *Biochemistry 35*, 11596−11604.
56. von Hippel, P. H., and Wong, K.-Y. (1965) *J. Biol. Chem. 240*, 3909−3923.
57. Moczygemba, C., Guidry, J., and Wittung-Stafshede, P. (2000) *FEBS Lett. 470*, 203−206.
58. Myers, J. K., Pace, C. N., and Scholtz, J. M. (1995) *Protein Sci. 4*, 2138−2148.
59. Falzone, C. J., Wang, Y., Vu, B. C., Scott, N. L., Bhattacharya, S., and Lecomte, J. T. J. (2001) *Biochemistry 40*, 4879−4891.
60. Pfeil, W. (1993) *Protein Sci. 2*, 1497−1501.

BI026005L